

Quantitative Study of the Decomposition of Dimethyl Methylphosphonate (DMMP) on Metal Oxides at Room Temperature and Above

Viktor N. Sheinker and Mark B. Mitchell*

Department of Chemistry, Clark Atlanta University, Atlanta, Georgia 30314

Received August 17, 2001. Revised Manuscript Received November 30, 2001

The adsorption and decomposition reactions of dimethyl methylphosphonate (DMMP) on a commercial γ -Al₂O₃, a γ -Al₂O₃-supported iron oxide, and a sol-gel-prepared alumina have been examined at temperatures from 25 to 400 °C. The capacities of these solids for the decomposition of DMMP have been measured, and the identities and amounts of the decomposition products determined over the entire temperature range. The alumina surfaces yield higher total amounts of decomposition products than the supported iron oxide material, with the sol-gel alumina showing very high activity. When corrected for surface area, however, the supported iron oxide material shows an activity equal to that of the γ -Al₂O₃ support. The sol-gel alumina shows a higher activity at all temperatures up to saturation of the surface, presumably because of the presence of transitional phases that yield more reactive surface sites. At 25 °C, the commercial γ -Al₂O₃ shows a total decomposition capacity of 117 μ mol/g, the alumina-supported iron oxide material a capacity of 93 μ mol/g, and the sol-gel alumina a capacity of 208 μ mol/g. At 100 °C, these capacities increase by about a factor of 3, and at 200 °C and above, all of the materials show some capacity for sustained decomposition of DMMP.

Introduction

The interactions and reactions of dimethyl methylphosphonate (DMMP) on a variety of surfaces have been studied by a number of research groups. DMMP generates significant interest because it is a relatively nontoxic compound that widely serves as a simulant for pesticides and chemical warfare agents.

Much of the work on DMMP decomposition has focused on trying to find or create active decomposition materials, primarily for application in chemical weapons disposal, which allows for the possibility of high-temperature reactions.¹ Weller and co-workers examined platinum-on-alumina materials for catalytic decomposition of DMMP.^{2,3} These materials are extremely active for DMMP decomposition, showing virtually stoichiometric conversion of DMMP to CO₂ plus phosphates for extended periods of time (>50 h) at temperatures as low as 250 °C. Lee et al.⁴ studied the efficiency of Cu-substituted hydroxyapatites as a low-cost alternative to the platinum catalysts. Cao et al.⁵ studied the thermocatalytic oxidation of DMMP on alumina-supported nickel, iron, copper, and vanadium and on silica and titania-supported vanadium. They found that, at temperatures of 400 °C and above, the silica-supported

vanadium catalyzed a very efficient decomposition reaction that was not poisoned by P₂O₅, proposed to account for the loss of activity on the other solids.

A significant need exists, however, for materials that will decompose chemical weapons at ambient temperatures in the absence of water for the protection of personnel in the field who may have been exposed to such agents. While several authors have discussed the decomposition of DMMP on alumina and on Fe₂O₃ at low temperatures, no published references exist that quantify the decomposition of DMMP on oxide materials at temperatures lower than 100 °C.

Templeton and Weinberg^{6,7} were among the first to investigate the surface chemistry of DMMP on aluminum oxide, using inelastic electron-tunneling spectroscopy, a surface vibrational spectroscopy, and proposed a mechanism for the decomposition of DMMP on this surface and found that decomposition of DMMP occurred at temperatures as low as 25 °C. White and co-workers⁸ examined the adsorption of DMMP on silica and on iron oxide using temperature-programmed desorption and Auger electron spectroscopy. They found that while α -Fe₂O₃ is active for decomposition of DMMP at temperatures as low as -23 °C, SiO₂ was found to be only slightly reactive and then only for the heavily hydrated form. Aurian-Blajeni and Boucher examined the interactions of DMMP with a variety of metal oxide surfaces using diffuse reflectance FT-IR methods, but

* To whom correspondence should be addressed. E-mail: mmitchel@cau.edu.

(1) Ekerdt, J. G.; Klabunde, K. J.; Shapley, J. R.; White, J. M.; Yates, J. T., Jr. *J. Phys. Chem.* **1988**, *92*, 6182.

(2) Graven, W. M.; Weller, S. W.; Peters, D. L. *Ind. Eng. Chem. Process Des. Dev.* **1966**, *5*, 183.

(3) Tzou, T. Z.; Weller, S. W. *J. Catal.* **1993**, *146*, 370.

(4) Lee, K. Y.; Houalla, M.; Hercules, D. M.; Hall, W. K. *J. Catal.* **1994**, *145*, 223.

(5) Cao, L.; Segal, S. R.; Suib, S. L.; Tang, X.; Satyapal, S. *J. Catal.* **2000**, *194*, 61.

(6) Templeton, M. K.; Weinberg, W. H. *J. Am. Chem. Soc.* **1985**, *107*, 97.

(7) Templeton, M. K.; Weinberg, W. H. *J. Am. Chem. Soc.* **1985**, *107*, 774.

(8) Henderson, M. A.; Jin, T.; White, J. M. *J. Phys. Chem.* **1986**, *90*, 4607.

were unable to observe decomposition on any of the oxides, including Al_2O_3 and MgO .⁹

Klabunde and co-workers^{10–13} were the first to examine the use of nanoscale oxide powders for the decomposition of DMMP. The use of nanosized particles of metal oxides has been pursued because these materials, depending on their mode of synthesis, contain a higher density of surface defect sites, sites that are intrinsically more reactive, than do larger sized particles of the same oxides.¹² However, no DMMP decomposition was observed at temperatures below 170 °C, and the majority of the work has been carried out at 500 °C.

Additionally, oxides whose surface reactivity can be activated by light, such as titania or amorphous manganese oxide, have been investigated for their ability to decompose DMMP. Obee and Satyapal examined the photocatalytic decomposition of DMMP on titania,¹⁴ and they were able to determine the photoinduced decomposition rate of DMMP on titania as well as the reaction products formed in the presence of oxygen. Segal et al.¹⁵ measured the photoassisted decomposition of DMMP on amorphous manganese oxide and found that the mechanism of decomposition was due, at least in part, to a photoassisted process.

Our previous studies of the decomposition of DMMP on metal oxide surfaces have focused on the surface chemistry and the decomposition pathways that occur on different oxides. These studies used infrared diffuse reflectance spectroscopy as a tool for the direct examination of the decomposition reaction.^{16,17} In our initial work, the species formed upon adsorption of DMMP on alumina, magnesia, iron oxide, and lanthanum oxide were examined as a function of temperature.¹⁶ The initial adsorption of molecular DMMP and the subsequent stepwise loss of the methoxy groups with increasing temperature were easily followed by observing the infrared absorption spectra of the surface species. In these earlier studies, it was shown that, for DMMP adsorbed on aluminum oxide, by 200 °C (100 °C for magnesium oxide and lanthanum oxide) the adsorbed DMMP has lost one methoxy group, which reacts with surface hydroxy groups to form methanol that evolves from the surface, and a surface-bound methyl methylphosphonate. Further heating to 300 °C results in the loss of the second methoxy group, forming a second methanol molecule, and an adsorbed methylphosphonate species. From those studies, it became clear that iron oxide behaved differently from other metal oxides. The iron oxide surface showed measurable decomposition of DMMP at lower temperatures than did the other oxides. Even more interesting was that iron oxide showed the ability to cleave the phosphorus–carbon

bond, a bond that was very resistant to cleavage on the other oxide surfaces. Our subsequent study of iron oxide supported on aluminum oxide showed that, at iron loadings above a certain threshold value, the material exhibited decomposition of DMMP upon adsorption at 25 °C, and the decomposition involved cleavage of the phosphorus–carbon bond.¹⁷

In the current study, three different metal oxides were examined for their relative activities and capacities for the decomposition of DMMP at temperatures from 25 to 400 °C, using quantitative FT-IR determination of gas-phase products in real time to monitor the products. The product flow curves were then integrated to determine the total decomposition capacity and the branching ratios. Each of the materials that was examined had been shown to exhibit some capacity for decomposition at ambient temperatures in earlier studies. The first to be examined was γ -alumina because the surface chemistry of DMMP adsorbed on this surface was thought to be well-understood.⁶ The second metal oxide studied was the alumina-supported iron oxide, whose surface chemistry had been found to be significantly different from that of alumina in our previous study and which we showed to be active for DMMP decomposition at room temperature. The final material to be studied was an alumina material synthesized using sol–gel methods that formed an alumina with a much higher surface area than the commercial γ -alumina. This study establishes a baseline for the reactivity of solids for the decomposition of DMMP at ambient temperatures and follows the changes in the decomposition that occur as a function of temperature, leading to the catalytic decomposition that occurs at high temperatures.

Experimental Section

The helium used for the study was a 99.9995% ultra-high-purity grade from Holox. DMMP was purchased from Aldrich and distilled under vacuum before use. All solids for the reaction studies are pretreated by heating in flowing O_2 for 1 h at 470 °C followed by heating in flowing He at 470 °C for 1 h. The sample was then cooled to the reaction temperature in flowing He.

The γ - Al_2O_3 used was a 99.995% pure material from Goodfellow, with an average particle size <100 nm. The alumina-supported iron oxide material was prepared as described previously.¹⁷ The particular material examined corresponded to the material that exhibited the unusual surface chemistry seen in the earlier work, with an iron loading of 11.6 wt % Fe (as Fe, not Fe_2O_3). Briefly, ≈ 2.20 g of iron(III) acetylacetonate, $\text{Fe}(\text{acac})_3$, from Aldrich was dissolved in 100.0 mL of acetonitrile (Fisher). Then, 5.0 g of γ -alumina was added to the solution and the mixture stirred at room temperature for 24 h. The solid was filtered from the solution, washed with clean solvent, dried in air, and then calcined at 500 °C in air for 24 h. The calcined solid was placed back into the $\text{Fe}(\text{acac})_3$ /acetonitrile solution, into which additional $\text{Fe}(\text{acac})_3$ had been added to bring the $\text{Fe}(\text{acac})_3$ concentration back to the initial value, and the impregnation procedure repeated. Approximately 20% of the iron complex was adsorbed from the solution by the substrate during each step. This process was repeated as needed to obtain the desired concentration of iron on the alumina support. The iron content of the material was determined by Galbraith Laboratories, Knoxville, TN.

The sol–gel alumina was prepared by adding excess amounts of NH_4OH to a solution of $\text{Al}(\text{NO}_3)_3$ with stirring until the pH was ≈ 10 –12. The gel precipitate of $\text{Al}(\text{OH})_3$ was separated from the liquid phase using a centrifuge. The liquid was decanted and the solid was resuspended in deionized water,

(9) Aurian-Blajeni, B.; Boucher, M. M. *Langmuir* **1989**, *5*, 170.

(10) Li, Y. X.; Schlup, J. R.; Klabunde, K. J. *Langmuir* **1991**, *7*, 1394.

(11) Li, Y. X.; Klabunde, K. J. *Langmuir* **1991**, *7*, 1388.

(12) Li, Y. X.; Koper, O.; Atteya, M.; Klabunde, K. J. *Chem. Mater.* **1992**, *4*, 323.

(13) Jiang, Y.; Decker, S.; Mohs, C.; Klabunde, K. J. *J. Catal.* **1998**, *180*, 24.

(14) Obee, T. N.; Satyapal, S. *J. Photochem. Photobiol. A* **1998**, *118*, 45.

(15) Segal, S. R.; Suib, S. L.; Tang, X.; Satyapal, S. *Chem. Mater.* **1999**, *11*, 1687.

(16) Mitchell, M. B.; Sheinker, V. N.; Mintz, E. A. *J. Phys. Chem. B* **1997**, *101*, 11192.

(17) Tesfai, T. M.; Sheinker, V. N.; Mitchell, M. B. *J. Phys. Chem. B* **1998**, *102*, 7299.

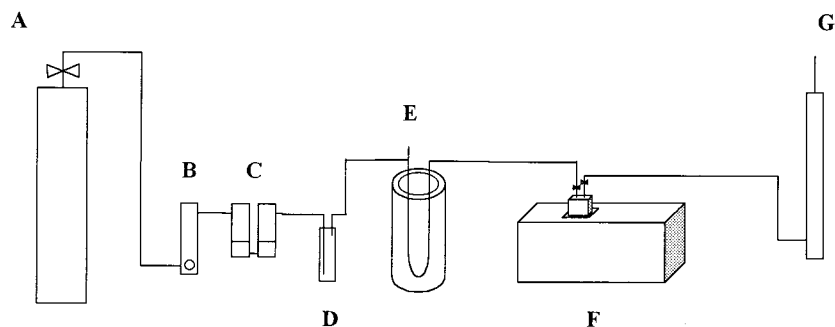


Figure 1. Schematic of microreactor experiment: (A) gas tank and regulator, (B) Manostat flow controller, (C) bubbler for DMMP, (D) aerosol trap, (E) $\frac{1}{4}$ -in. u-tube microreactor, (F) Magna 750 FT-IR with Infrared Analysis 2.4PA gas cell, and (G) gas flow bubblemeter.

centrifuged again, the liquid decanted, the solid resuspended, and so forth, until the pH was neutral. The precipitate was dried at 80 °C at atmospheric pressure and then heated in a vacuum to 125 °C. The dried material was then calcined at 500 °C in air for 24 h.

The microreactor system (see Figure 1) consists of a $\frac{1}{4}$ in. o.d. stainless steel u-tube in a controlled-temperature furnace (Hoskins, Type FA120 electric furnace, coupled to an Omega Engineering Model CN 3202-TC1 process control unit). The microreactor is connected to a gas inlet system that carries the DMMP/He mixture to the reactor and an exit system that carries the products to an infrared gas cell for analysis. High-purity perfluoroalkoxy tubing is used throughout the system to minimize adsorption of the gases. The helium gas bubbles through liquid DMMP, in a specially fabricated two-stage bubbler, at a flow rate of 30 mL/min. After the bubbler, the DMMP/He stream passed through a flow-through glass wool trap, previously saturated with DMMP vapor, to remove any DMMP aerosol. The flow of DMMP was calibrated by directing the flowing gas mixture, after the bubbler and the aerosol trap, to a small glass condensation vessel specifically designed for collecting volatile compounds. This small vessel was placed in liquid nitrogen to trap the DMMP flowing through it. The vessel was weighed before the experiment and after 10–12 h collection time, and the difference in mass was determined. The experiment was repeated several times with the result that the DMMP concentration in the He stream was calculated to be 30.25 $\mu\text{mol/L}$. At a flow rate of 30.0 mL/min, the flow rate of DMMP was determined to be 0.908 $\mu\text{mol/min}$.

For reaction studies, the adsorbent (≈ 60 mg) was placed near the bottom of the “u” but on the entrance side, with a small plug of glass wool, shown to be inert to DMMP in the blank experiments, used to support the adsorbent bed. Because the adsorbent consisted of such small particles, the adsorbent was mixed with ≈ 100 mg of glass wool, cut into ≈ 2 -mm pieces, before it was placed in the reactor, to help maintain gas flow through the bed. A type K thermocouple in the adsorbent bed provided the temperature feedback to the Omega process control unit.

After the adsorbent bed, the gas stream flowed to a long-path gas cell (Ultra-Mini Long Path Cell from Infrared Analysis, Inc.) with an effective path length of 2.4 m and an internal volume of 100 mL. Infrared spectra, at 2-cm⁻¹ resolution, were collected approximately every 2 min. The infrared responses for the different products (CH₃OH, (CH₃)₂O, CO, CO₂, and CH₄) were calibrated using premixed, certified gas mixtures containing each gas individually in helium purchased from Matheson Gas or Holox, varying the pressure inside the cell to adjust the concentration over an appropriate range, integrating the infrared absorption profiles, and fitting the integrated intensities as a function of concentration to Beer’s Law. Overlap of DMMP infrared absorptions with those of the product gases were dealt with by using a DMMP band that did not overlap any of the product absorptions to provide an internal standard to guide the subtraction of the overlapping DMMP component from the product absorptions. This was not a significant problem except for DMMP overlap with

the methanol absorption at low temperatures, and this is discussed later.

The breakthrough point (BTP) of DMMP for each adsorbent at each temperature was determined by extrapolating a plot of the DMMP integrated infrared absorption intensity (1297–1240 cm⁻¹) vs μmol of DMMP passed through the sample to zero intensity.

The concentrations of the gases measured in the infrared cell are not true representations of the concentrations in the gas stream coming into the cell from the reactor. The concentrations coming from the reactor were determined by setting up the differential equation describing the changing gas concentration in the cell, a simple mixing problem, assuming instantaneous mixing in the gas cell.

$$\frac{dC_{\text{cell}}}{dt} = \frac{fC_{\text{in}}}{V} - \frac{fC_{\text{cell}}}{V} \quad (1)$$

where f is the flow rate, C_{cell} is the measured concentration in the cell, C_{in} is the concentration coming into the cell from the reactor, and V is the volume of the cell.

Integrating this expression and rearranging yields

$$C_{\text{in}} = \frac{C_{\text{cell},t_2} - C_{\text{cell},t_1}e^{-(fV)(t_2-t_1)}}{1 - e^{-(fV)(t_2-t_1)}} \quad (2)$$

With eq 2, an average concentration coming into the gas cell between two measurement times, t_1 and t_2 , can be determined. In the plots that follow, the calculated value for each C_{in} is assumed to correspond to the concentration at the midpoint between t_2 and t_1 .

Results

Blank Experiments. Several blank experiments were performed to determine the effective volume of the reactor and tubing leading up to the analysis cell. These experiments were identical in all ways to the decomposition experiments except that no adsorbent was placed in the microreactor. The results were found to be slightly temperature-dependent, presumably due to adsorption of DMMP on the walls of the u-tube and the glass wool in the reactor at low temperatures. All of the graphs presented in the following sections have been corrected for the effective volume of the reactor and tubing. Additionally, several blank experiments were conducted using a mixture of methanol in helium (1000 ppm) to determine the transport rate of methanol relative to that of DMMP through the tubing. These experiments showed that there was no difference, within experimental error, in the transport rates of these two gases through the tubing. Blank experiments using dimethyl ether, CO,

Table 1. Summary of the Experimental Results^a

solid	temp/°C	induction period/ μmol of DMMP(± 5)	max. total flow rate of volatile carbon products/ $\mu\text{mol min}^{-1}$ (± 0.02)	point of max. product flow rate/ μmol of DMMP (± 5)	total volatile carbon produced/ μmol (± 1) ($\mu\text{mol g}^{-1}$)	breakthrough point (BTP)/ μmol of DMMP(± 10)	total volatile carbon produced at BTP/ μmol (± 1)
$\gamma\text{-Al}_2\text{O}_3$	25	38	0.25	62	7(117)	49	0.46
	100	10	0.58	36	19.5(325)	42	14.3
	200	0	0.92	36	59.5(992) ^b	41	27.3
	300	0	1.49	43	210(3.48×10^3) ^b	75	99.9
	400	0	1.92	110	625(10.4×10^3) ^b	135	248
$\text{FeO}_x/\text{Al}_2\text{O}_3$	25	37	0.46	48.9	5.6(93)	53	4.1
	100	5	0.67	36	21.5(350)	38	10.4
	200	0	0.83	37	33.7(562) ^b	45	18.2
	300	0	1.83	45	176(2.93×10^3) ^b	61	79.1
	400	0	2.26	89	585(9.75×10^3) ^b	102	174
sol-gel Al_2O_3	25	93	0.23	153	12(208)	175	11.8
	100	1	1.28	34	40(667)	39	31.5
	200	0	1.42	63	99.7(1.66×10^3) ^b	67	68.8
	300	0	2.90	84	452(7.53×10^3) ^b	99	215
	400	0	2.64	176	821(13.7×10^3) ^b	202	450

^a Estimated experimental uncertainties are shown for the various quantities in the table headings. The listed uncertainties are for the lower values of the various quantities. The minimum estimated uncertainty is $\pm 5\%$. ^b Values at $3 \times$ BTP.

Adsorption and Decomposition of DMMP on $\gamma\text{-Al}_2\text{O}_3$ at 25 °C

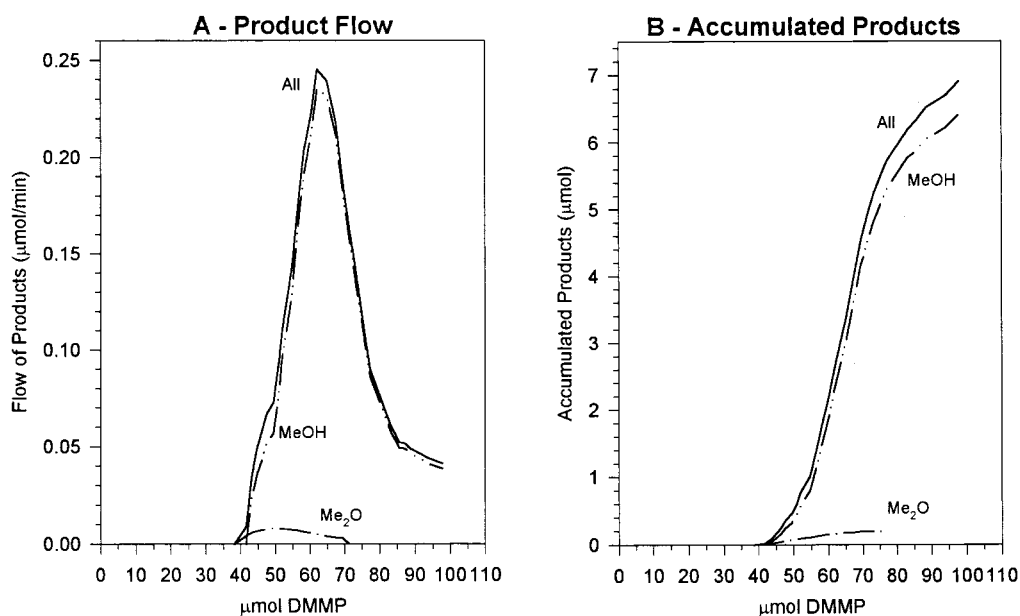


Figure 2. Results from the decomposition of DMMP on γ -alumina at 25 °C. "All" represents the number of $\mu\text{mol}/\text{min}$ (or μmol) of carbon that appears as volatile products in this figure equal to 2 times the number of $\mu\text{mol}/\text{min}$ (or μmol) of dimethyl ether plus the number of $\mu\text{mol}/\text{min}$ (or μmol) of methanol.

and CH_4 showed that these gases had only slightly faster transport rates through the tubing.

Table 1 below summarizes several of the important aspects of the experimental results. In the following sections, results from individual experiments are detailed, emphasizing the differences in behavior of the three solids examined and the methods used to analyze the results.

γ -Alumina. Room-Temperature Adsorption. The measured reaction products from the room temperature study of γ -alumina are shown in Figure 2. The accumulated flow of DMMP through the adsorbent bed, in micromoles, is the horizontal axis in the plots. This has been corrected for the volume of the reactor and tubing as discussed in the Experimental Section. The

vertical axis corresponds to the flow rate of the products observed ($\mu\text{mol}/\text{min}$), Figure 2A, or to the total accumulated flow of volatile carbon species produced by the reaction (μmol), Figure 2B. ("All" represents the total number of micromoles of carbon produced by the reaction that appeared as volatile products, equal to 2 times the flow of dimethyl ether plus the flow of methanol at this temperature). As can be seen in Figure 2A, dimethyl ether was observed first at the infrared cell, beginning at $\approx 38 \mu\text{mol}$ of DMMP. Figure 2B shows the accumulated product formation as a function of DMMP flow and represents the integration of Figure 2A.

There is a noticeable induction period prior to observation of reaction products, corresponding to a flow of $38 \mu\text{mol}$ of DMMP. The induction period is due to

Breakthrough of DMMP γ -Al₂O₃ at 25 °C

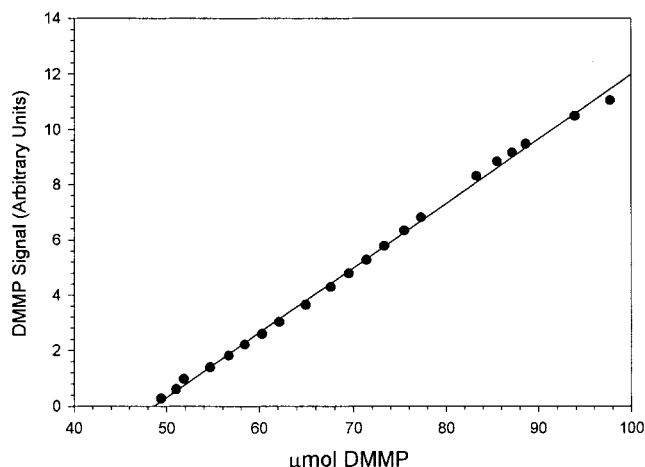


Figure 3. Breakthrough curve for DMMP flowing through γ -alumina at 25 °C.

adsorption of methanol and dimethyl ether onto the surface of the adsorbent. The measured product flow from the reactor is a convolution of the rate of product formation with the transport of the products through the adsorbent bed.

Figure 3 shows the breakthrough curve for DMMP. The vertical scale corresponds to the intensity of the integrated DMMP band. DMMP enters the infrared cell as a vapor but accumulates on the interior surfaces of the cell, including the mirrors, since they are not heated. As a result, the intensity of the integrated band grows quickly and cannot be used to quantify the DMMP concentration in the cell. This curve and similar ones for all the materials and temperatures studied are simply used to determine the breakthrough point (BTP) of DMMP through the adsorbent bed.

At the low temperatures, due to the relatively low degree of decomposition, the breakthrough of DMMP causes some difficulties in the determination of the methanol concentration. The methanol band used for quantifying its concentration overlaps a strong DMMP absorption. A DMMP band that does not overlap those of any of the reaction products is used to determine the DMMP contribution to the overlapped band. This DMMP contribution is subtracted from the observed band, and the resulting band is integrated to determine the methanol concentration. This method works well, even when the DMMP contribution becomes large compared to that of methanol. However, at low temperatures when the methanol production drops to low levels and almost none of the inlet DMMP is being decomposed, the absolute error in the methanol determination becomes significantly greater than the concentration. It is at this point that the data are no longer recorded in the product flow curves.

100 °C Adsorption. At 100 °C, much more dimethyl ether was produced, and initially it was the only product observed (see Figure 4). A significantly shorter induction period is observed at 100 °C than was seen at 25 °C, and the breakthrough point (BTP) of DMMP was found to be 42 μ mol of DMMP, a somewhat lower number than that for room temperature. Both of these observations are consequences of the extra thermal energy available

at 100 °C that lowers the capacity of the material for molecular adsorption.

200 °C Adsorption. At 200 °C, no induction period was found prior to observation of reaction products at the infrared cell, indicating little adsorption of the reaction products on the adsorbent. Approximately 20% of the inlet DMMP continued to be decomposed after a flow of 140 μ mol of DMMP, well after the observed BTP of 41 μ mol of DMMP. This sustained reaction is most likely due to reaction of inlet DMMP with adsorbed DMMP species, which at this temperature are almost certainly DMMP fragments left after cleavage of one of the methoxy groups.

300 °C Adsorption. Methanol and dimethyl ether were again observed at the infrared cell with no induction period. Breakthrough of DMMP occurred after exposure to 75 μ mol of DMMP. At the BTP, a total of 99.9 μ mol of volatile carbon had been produced, corresponding to between one and two methoxy groups removed per molecule of DMMP. Evidence for both methoxy groups being removed at these temperatures has been seen in previous work from this laboratory.¹⁶ After the BTP, methanol continued to be produced in significant amounts, equal to decomposition of about 75% of the inlet DMMP. Even after a flow of 240 μ mol of DMMP, nearly 60% of the inlet DMMP continued to be decomposed.

400 °C Adsorption. Figure 5 shows the results from the adsorption/decomposition experiment carried out at 400 °C. By this temperature a second reaction pathway has become available, involving the production of CO₂, CO, and CH₄. These products may be formed from methanol rather than from DMMP directly. As a check on this possibility, a similar experiment was carried out using methanol as the reactant gas. When γ -alumina was exposed to methanol alone in flowing helium at 350 °C (0.7 μ mol/min), CO and CH₄ were produced (\approx 0.15 μ mol/min for each), along with smaller amounts of dimethyl ether (\approx 0.06 μ mol/min), while at 250 °C, only dimethyl ether was observed.

DMMP breakthrough was observed after a flow of 135 μ mol of DMMP, just at the point where the methanol production was observed to turn on and the production of the other products ceased. Prior to breakthrough, beginning after a flow of \approx 75 μ mol of DMMP, an increase in the product flow is observed that peaks just before breakthrough. This peak coincides with the flow of methanol from the reactor. The adsorption and decomposition reaction of DMMP is very efficient on the alumina surface at these temperatures. We believe that the front of molecular DMMP, as it moves through the adsorbent bed, reacts with or replaces decomposition products that have adsorbed on the alumina surface. Possible products include adsorbed methoxy or hydroxyl groups. One possibility is that DMMP reacts with adsorbed methoxy groups to yield dimethyl ether. A second possibility is that an increased concentration of surface hydroxyl groups, from the dehydration reaction that forms dimethyl ether from methanol, leads to a temporary increase in the rate of methanol production. Both of these possibilities could help explain the observed increase in the rate of product flow. Similar behavior was observed for all the materials examined, most obviously at 300 and 400 °C. The BTP marked a

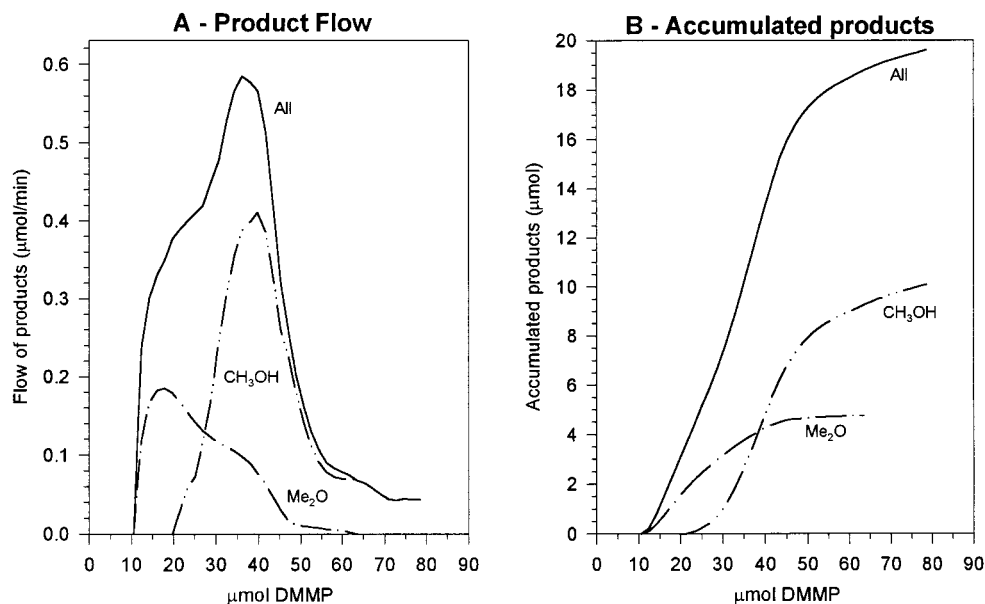
Adsorption and Decomposition of DMMP on $\gamma\text{-Al}_2\text{O}_3$ at 100 °C

Figure 4. Product flow and accumulated product curves for DMMP decomposing on γ -alumina at 100 °C.

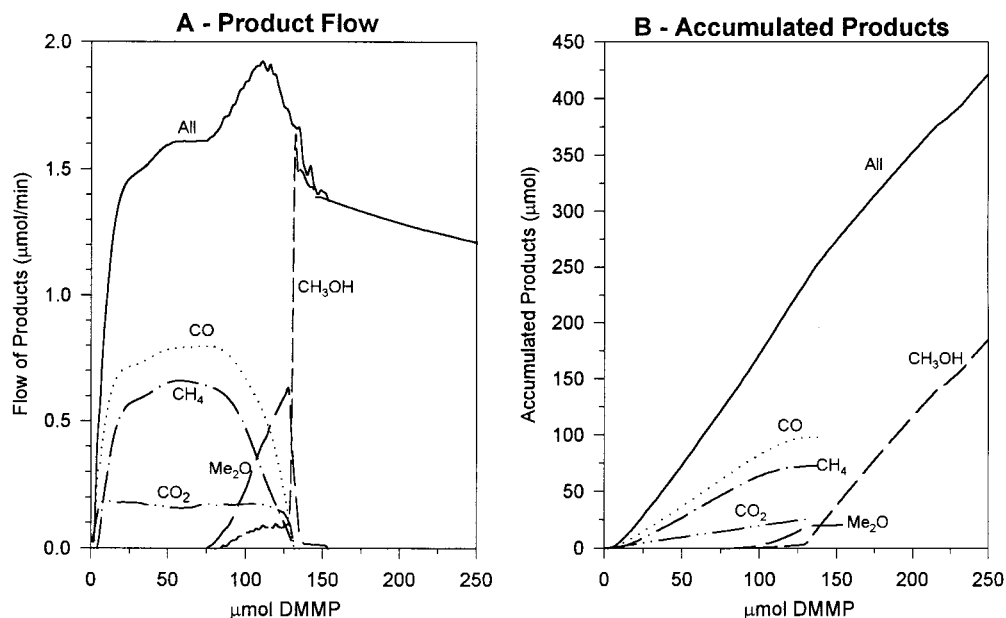
Adsorption and Decomposition of DMMP on $\gamma\text{-Al}_2\text{O}_3$ at 400 °C

Figure 5. Product flow and accumulated product curves for DMMP decomposing on γ -alumina at 400 °C.

distinct change in the products observed and, by extension, to the types of reaction sites available.

Iron Oxide Supported on Alumina ($\text{FeO}_x/\gamma\text{-Al}_2\text{O}_3$). The experimental method used to prepare this material was designed to result in a well-dispersed layer of iron species on the $\gamma\text{-Al}_2\text{O}_3$ surface. The acetylacetonate ligands on the iron oxide precursor prevent formation of clusters of iron oxide. It is possible that a spinel phase, FeAl_2O_4 (hercynite), was formed, and this may well have been the major form of the surface iron formed in the initial steps of the impregnation procedure. The material examined in the current study was formed by seven successive impregnations. This same material was examined in an earlier published study and was found to cleave DMMP at room temperature via cleavage of the P-CH₃ bond.¹⁷ However, X-ray diffraction studies

of this material showed no evidence for formation of either a separate spinel phase or an Fe_2O_3 , hematite, phase. For the purposes of the current discussion, the material will be designated as $\text{FeO}_x/\text{Al}_2\text{O}_3$.

Room-Temperature Adsorption. At room temperature, the maximum product flow rate was almost twice that observed for aluminum oxide at the same temperature (Figure 6), indicating that either the decomposition rate on the $\text{FeO}_x/\text{Al}_2\text{O}_3$ surface is faster than on the $\gamma\text{-Al}_2\text{O}_3$ surface or that methanol does not adsorb as strongly on $\text{FeO}_x/\text{Al}_2\text{O}_3$ as on $\gamma\text{-Al}_2\text{O}_3$. The induction period found for this surface, corresponding to 37 μmol of DMMP, is almost identical to that of $\gamma\text{-Al}_2\text{O}_3$ at the same temperature. Though the maximum product flow rate was higher for the supported iron oxide, the total amount of accumulated products was observed to be

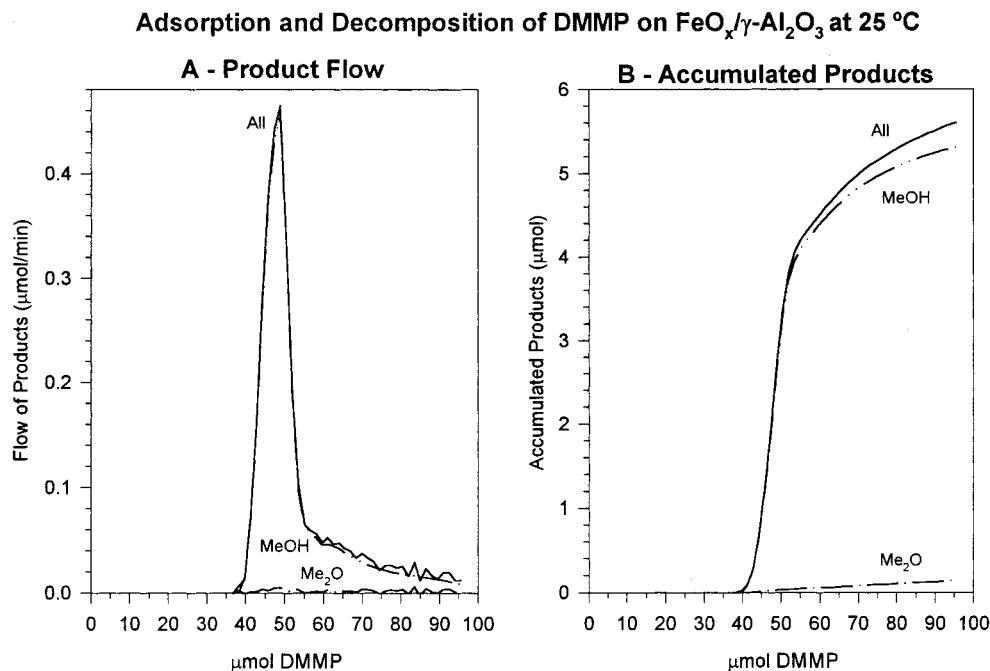


Figure 6. Product flow and accumulated product curves from the decomposition of DMMP on FeO_x/Al₂O₃ at 25 °C.

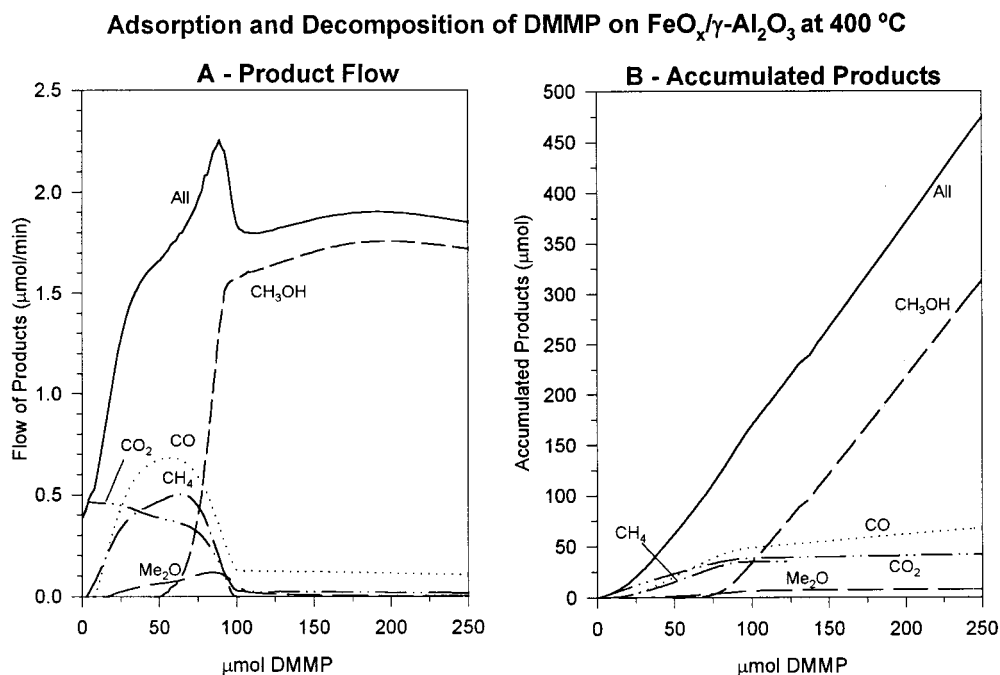


Figure 7. Product flow and accumulated product curves from the decomposition of DMMP on FeO_x/Al₂O₃ at 400 °C.

somewhat less than that for aluminum oxide; 5.5 μmol of volatile carbon products was formed by the supported iron oxide while about 6.8 μmol of volatile carbon products was formed by aluminum oxide. This difference may be accounted for by the lower surface area as discussed later because the surface area of the supported iron oxide was determined to be ≈30% less than that of the γ-alumina (106 m²/g). Only traces of dimethyl ether were formed by the supported iron oxide. Breakthrough of DMMP occurred only after the methanol flow was nearly over, after a flow of 53 μmol of DMMP, in contrast to the behavior found for γ-alumina.

Adsorption at Temperatures above Ambient. The same general trend was observed as a function of temperature for the FeO_x/Al₂O₃ material as was observed for the

commercial γ-Al₂O₃. This material is, however, a more active oxidation catalyst than is alumina itself. At 200 °C, CO₂ was the first product observed, and the initial production level corresponded to about one-third of the inlet DMMP concentration. Shortly thereafter, dimethyl ether and then methanol were observed. At 300 °C, carbon dioxide and carbon monoxide were the first products observed from the DMMP decomposition, followed shortly by dimethyl ether. Breakthrough of DMMP was observed to occur after exposure to 61 μmol of DMMP, and the total volatile carbon produced up to breakthrough was 79 μmol. This corresponds to more than one volatile carbon species produced per molecule of DMMP. After the BTP, the rate of product flow was 0.67 μmol/min and was virtually constant for the dura-

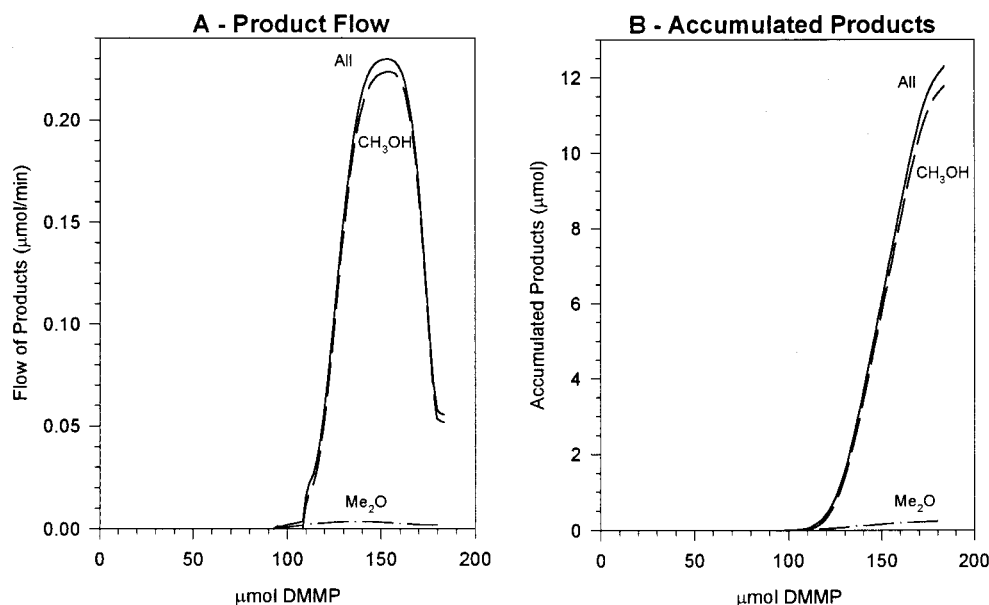
Adsorption and Decomposition of DMMP on Sol-Gel Al_2O_3 at 25 °C

Figure 8. Product flow and accumulated product curves from the adsorption of DMMP on the sol-gel alumina formulation at 25 °C.

tion of the experiment, out to 200 μmol of DMMP. The only product observed after the BTP was methanol. This rate represents decomposition of about 75% of the inlet DMMP.

For the DMMP decomposition reaction at 400 °C, CO_2 , CO, CH_4 , methanol, and dimethyl ether were all observed as products (Figure 7). CO_2 was observed instantly from the reactor, followed by CO and CH_4 along with smaller amounts of dimethyl ether. Breakthrough of DMMP occurred after a flow of 102 μmol of DMMP and occurred simultaneously with the end of CH_4 production, followed closely by the end of dimethyl ether formation. Methanol replaced these two products in the product flow stream. CO continued to be produced, though at much lower concentrations than before breakthrough. Sustained product flow at a rate of about 1.6 $\mu\text{mol}/\text{min}$ continued for the duration of the experiment, to a flow of 400 μmol of DMMP.

Sol-Gel Aluminum Oxide. Room-Temperature Adsorption. This alumina was determined to have a surface area of 253 m^2/g and as a result yielded a significantly higher capacity for DMMP. Figure 8 shows the product flow and accumulated product curves for this material at room temperature. Breakthrough of DMMP was found to occur after exposure to 175 μmol of DMMP, with the decomposition on this surface yielding more than 12 μmol of volatile carbon. The maximum rate of product flow observed for the sol-gel formulation was about the same as that observed for the γ -alumina, 0.23 $\mu\text{mol}/\text{min}$.

Adsorption at Temperatures above Ambient. At 100 °C, the sol-gel alumina was found to have a peak product flow rate of 1.3 $\mu\text{mol}/\text{min}$, nearly twice the rate observed for the alumina-supported iron oxide and more than twice the rate observed for the γ - Al_2O_3 . Breakthrough was observed after exposure to 39 μmol of DMMP, a much shorter exposure than found for the breakthrough at room temperature, again a consequence of the extra thermal energy available. The total

accumulated volatile carbon produced was ≈ 40 μmol , indicating a very high decomposition activity at this temperature.

At 200 °C, breakthrough of DMMP was observed after exposure to 67 μmol of DMMP. The total accumulated volatile carbon produced at the breakthrough point was found to be ≈ 69 μmol , corresponding almost exactly to one volatile carbon species produced per molecule of DMMP. The production of methanol continued after breakthrough, but fell to a value of about 0.2 $\mu\text{mol}/\text{min}$ after exposure to ≈ 130 μmol of DMMP.

At the BTP at 300 °C, which occurred after exposure to 99 μmol of DMMP, ≈ 215 μmol of volatile carbon products had been produced, corresponding to slightly more than two molecules of volatile carbon produced per molecule of DMMP. Methanol and dimethyl ether were the major products produced prior to breakthrough, along with minor amounts of carbon monoxide. After breakthrough, methanol was the only product observed, and the production of methanol slowly declined to a level of about 0.2 $\mu\text{mol}/\text{min}$ after exposure to 1000 μmol of DMMP.

At 400 °C, large amounts of CO and CH_4 were the initial products observed, in addition to small amounts of CO_2 , representing loss of two carbon atoms per molecule of DMMP. As their formation rate declined, the production of methanol and dimethyl ether was observed to increase (Figure 9). Breakthrough at 400 °C was not observed until after exposure to 202 μmol of DMMP, at which point 450 μmol of volatile carbon had been produced. Only methanol was observed in the product stream after breakthrough of DMMP, as was found for the reaction at 300 °C. The formation rate of methanol declined after breakthrough at 400 °C almost exactly as was observed at 300 °C, so that after exposure to 1000 μmol of DMMP, the flow of methanol was found to be only 0.2 $\mu\text{mol}/\text{min}$.

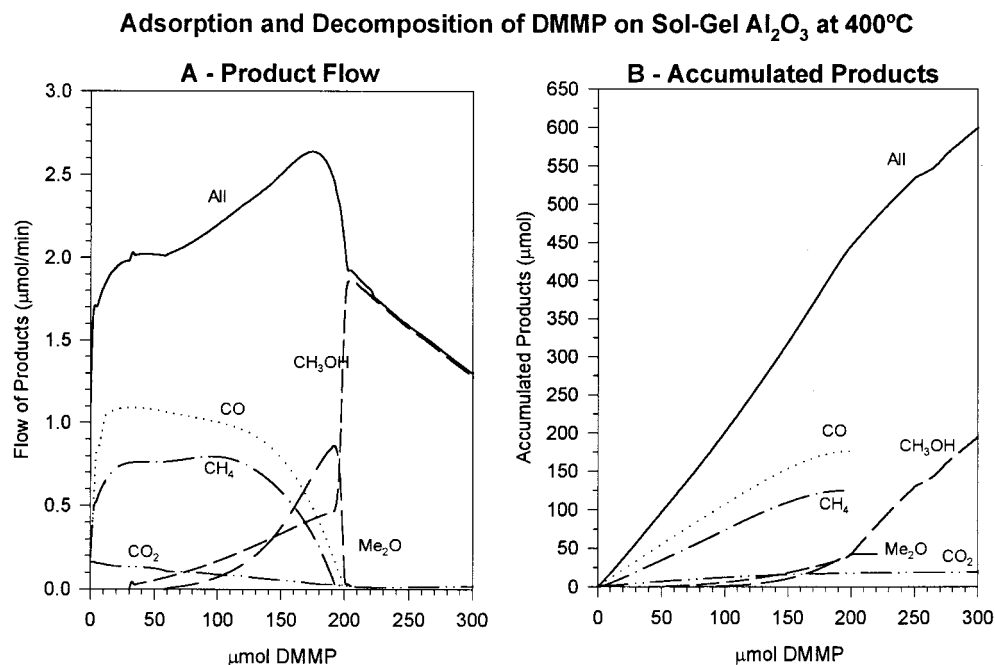
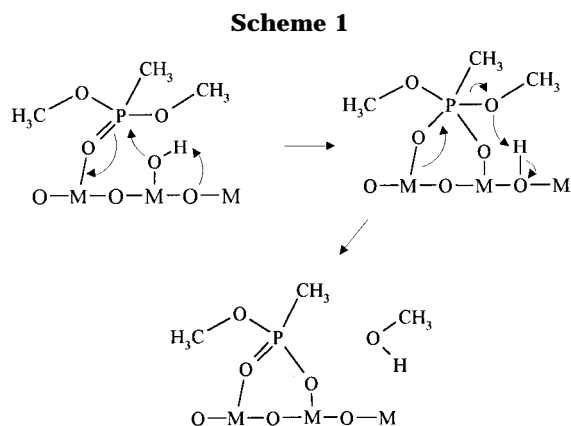


Figure 9. Product flow and accumulated product curves from the adsorption of DMMP on the sol-gel alumina formulation at 400 °C.



Discussion

Templeton and Weinberg, in their work on the adsorption of DMMP on alumina, found that DMMP can adsorb on the alumina surface on two different sites, both coordinated through the phosphoryl oxygen, either at surface hydroxyl (Brønsted acid) sites or at uncoordinated aluminum (Lewis acid) sites.⁶ Coordination at the Brønsted sites was found to yield only molecular adsorption while coordination at the Lewis acid sites leads to decomposition. The production of methanol from the adsorption of DMMP on alumina was proposed to proceed via the mechanism shown in Scheme 1. This reaction is an acid-catalyzed nucleophilic displacement reaction, with the Lewis sites on the surface catalyzing the displacement of the methoxy group, yielding adsorbed methyl methylphosphonate and a molecule of methanol. For aluminum oxide, at temperatures lower than 200 °C, a fraction (<1) of the surface adsorption sites are active for cleavage of one of the P–OCH₃ bonds, and the active fraction increases with increasing temperature. By 200 °C, virtually all of the adsorbed DMMP is in the form of methyl methylphosphonate, and after heating to 300 °C, most of the adsorbed DMMP molecules have lost both methoxy groups.^{6,16}

While the formation of methanol is accounted for in Scheme 1 directly from the decomposition of DMMP, the observed production of dimethyl ether requires a second step and can be accounted for in at least two different ways. Some of the methanol that is formed during the initial adsorption/decomposition of DMMP can re-adsorb at sites downstream and react with a second methanol molecule to form dimethyl ether and water, a reaction that was observed in independent experiments in our laboratory using methanol as the reactant gas. Alternatively, an adsorbed DMMP molecule could react with methanol to form dimethyl ether and a surface-bound DMMP fragment. The degree to which these processes occur decreases as DMMP reacts with and poisons the surface acid sites.

Our previous work has shown that, at temperatures of 200 °C and lower, DMMP loses no more than one methoxy group per molecule, on average.¹⁶ Between 200 and 300 °C, most oxides begin to promote cleavage of a second P–OCH₃ bond. Thus, in Table 1, the total number of micromoles of volatile carbon formed at temperatures of 200 °C and below is equal to the total number of micromoles of DMMP decomposed. It is instructive to compare the number of micromoles of DMMP decomposed at the breakthrough point to the total flow of DMMP at the BTP. For the sol-gel Al₂O₃ material at 200 °C, the amount of DMMP decomposed is approximately equal to the DMMP flow at the BTP, indicating that up until the BTP, every molecule of DMMP, on average, was decomposed to yield one methanol molecule (or 1/2 dimethyl ether molecule) and an adsorbed fragment. For the other solids and for the lower temperatures for the sol-gel Al₂O₃, the amount of DMMP decomposed is less than the DMMP flow at the BTP. This shows that, at temperatures less than 200 °C, much of the DMMP adsorption is molecular adsorption, even though significant decomposition does take place. At 300 °C and above, all the solids show more than one molecule of volatile carbon produced per

Specific Total Product Yield at Breakthrough vs Temperature

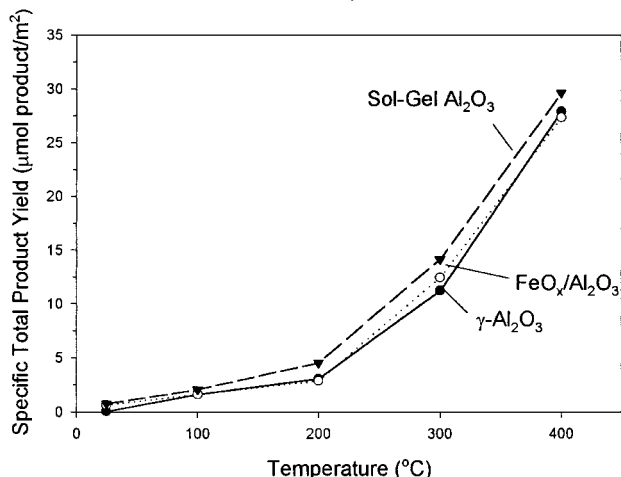


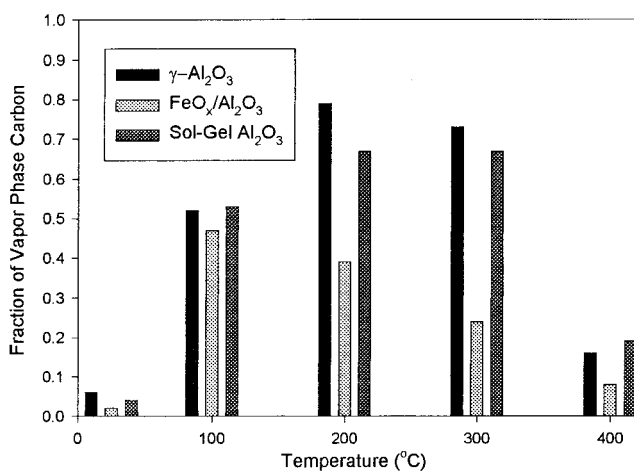
Figure 10. Graph of the specific total product yield at breakthrough (μmol of volatile carbon produced/ m^2 of surface area) as a function of temperature.

molecule of DMMP, indicating that a second P–O bond (or possibly, but less likely, the P–C bond) is being cleaved.

At temperatures <300 °C, the primary reaction products observed are dimethyl ether and methanol. The $\text{FeO}_x/\text{Al}_2\text{O}_3$ material produced CO and CO_2 at temperatures lower than the alumina materials, consistent with the properties of iron oxide as an oxidation catalyst. A small amount of CO_2 was observed to be produced by the iron oxide material at 200 °C, and at 300 °C, CO and CO_2 account for nearly one-third of the total products formed prior to the BTP. On all the solids prior to the BTP at 400 °C, the primary products observed are CH_4 , CO, and CO_2 .

Decomposition of DMMP Prior to the BTP. The analysis of the reactivity of the materials examined in the current study falls more or less naturally into two regimes: the reactivity of the surface itself and the sustained decomposition activity that continues after saturation of the surface. The analysis of the surface reactivity considers the total volatile products produced up until the point that DMMP breaks through the bed. In these experiments, the total product yield values at the BTP are indicative of the reactivity of the surface of the adsorbent. To remove the dependence of the reactivity on the surface area, the total product yield at the breakthrough point per square meter of surface area was determined. This value, which we have called the specific total product yield, was plotted as a function of temperature and is shown in Figure 10. Figure 10 demonstrates the relative reactivity of the surface sites as a function of temperature. The values for the $\gamma\text{-Al}_2\text{O}_3$ surface overlap those of the $\text{FeO}_x/\text{Al}_2\text{O}_3$ material, showing that these materials have reactivities that are very similar when surface area is taken into account, suggesting that the iron impregnation does little to enhance the average surface activity of the alumina, at least in terms of the formation of gas-phase products. The higher reactivity of the sol-gel formulation is probably due to the presence of transition alumina phases in the sol-gel alumina that have more reactive surface groups.

A - Branching Ratios - Dimethyl Ether



B - Branching Ratios - Methanol

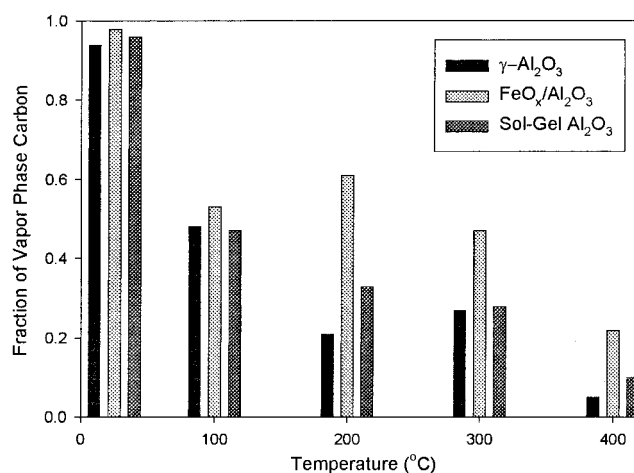


Figure 11. Branching ratios for the total accumulated formation of dimethyl ether and methanol as a function of temperature for the different materials at the BTP. Dimethyl ether is counted twice to account for the number of carbons per molecule. The estimated uncertainty in the mole fraction values is ± 0.05 .

The $\gamma\text{-Al}_2\text{O}_3$ and the sol-gel Al_2O_3 show very similar product distributions at all temperatures. The branching ratios for the accumulated formation of dimethyl ether and methanol, at the BTP, are shown in Figure 11. The branching ratios are calculated by dividing the total number of micromoles of the particular product formed up to the BTP (multiplied by two for dimethyl ether), by the total number of micromoles of volatile carbon produced. After the BTP, the dominant product in all cases is methanol. The likely source of dimethyl ether is via the acid-catalyzed dehydration of methanol, as mentioned above, with the surface providing the acid sites. Thus, the higher production of dimethyl ether by the alumina materials is consistent with these surfaces being more acidic than the $\text{FeO}_x/\text{Al}_2\text{O}_3$. At 400 °C, where the formation of CO, CO_2 , and CH_4 become important, the $\text{FeO}_x/\text{Al}_2\text{O}_3$ material forms more CO_2 and less CO than the alumina materials, with similar amounts of CH_4 formed as on the alumina surfaces. Table 2 shows the branching ratios for the formation of CO, CO_2 , and CH_4 , showing the more strongly oxidizing nature of the iron oxide material.

Table 2. Branching Ratios for the Formation of CO, CH₄, and CO₂^a

	CO		CH ₄		CO ₂	
	300 °C	400 °C	300 °C	400 °C	300 °C	400 °C
γ-Al ₂ O ₃	n.o.	0.39	n.o.	0.29	n.o.	0.10
FeO _x /Al ₂ O ₃	0.12	0.28	n.o.	0.20	0.17	0.22
sol-gel Al ₂ O ₃	0.04	0.39	n.o.	0.27	0.01	0.04

^a n.o.: not observed.

Table 3. Sustained Decomposition Reaction at Higher Temperatures (Rate of Product Flow in μmol/min)

	200 °C		300 °C		400 °C	
	2 × BTP ^a	3 × BTP	2 × BTP	3 × BTP	2 × BTP	3 × BTP
γ-Al ₂ O ₃	0.31	0.20	0.66	0.55	1.21	1.06
FeO _x /Al ₂ O ₃	0.10	0.064	0.67	0.65	1.90	1.80
sol-gel Al ₂ O ₃	0.19	0.10 ^b	1.16	0.83	0.84	0.36

^a BTP = breakthrough point. ^b Extrapolated value.

Sustained Decomposition. The second aspect of the reactivity of these materials is their sustained decomposition activity. At temperatures of 400 °C and below, all of the published studies of DMMP decomposition on solids except that of the Pt/Al₂O₃ material studied by Tzou and Weller³ have shown that the solids lose activity after some period of reaction. Even at 500 °C, Li and Klabunde¹¹ found that nanoscale MgO acts as a stoichiometric destructive adsorbent for DMMP, not a catalytic one, decomposing one DMMP molecule for every two MgO surface species. Once the initial decomposition step has occurred (see Scheme 1), the Lewis acid site is poisoned because there is no subsequent reaction step that results in the formation of a volatile phosphorus species, although continued loss of the carbon fragments does occur. The formation of an unreactive bulk phosphate species is usually proposed to account for deactivation of the decomposition reaction, although the P₂O₅ product that results from the decomposition reaction on vanadium supported on silica has been suggested to be an active participant in the continued decomposition observed at 400 and 500 °C.⁵

In this aspect of the decomposition reaction, the FeO_x/Al₂O₃ material is more active at higher temperatures than the other materials. In Table 3 are presented the product flow rates at two different times during the course of the reaction, at 200, 300, and 400 °C (sustained reactivity was insignificant at 100 °C and lower). Multiples of the breakthrough point were chosen to compare reactivity because these represent multiples of the surface saturation coverage for a particular surface at these temperatures. As can be seen in Table 3, the sol-gel alumina reactivity is apparently not as robust as that of the γ-Al₂O₃ or the FeO_x/Al₂O₃. While the reactivity of the surface of this material is significantly higher than that of the other two adsorbents, the reactivity decays rapidly after the BTP, especially at higher temperatures. The sustained reactivity of the commercial γ-Al₂O₃ relative to that of the sol-gel alumina may be explained by the recent study by Cao et al.⁵ in which those authors suggest that deactivation of the thermocatalytic activity of solids used for DMMP decomposition ultimately results from the formation of an inactive bulk phosphate. The higher surface area sol-gel alumina is converted to a bulk phosphate faster than the lower surface area γ-Al₂O₃. The sustained reactivity of the FeO_x/Al₂O₃ surface is extremely high

at 400 °C, representing the loss of two carbon atoms from each DMMP molecule entering the adsorbent bed, even well after saturation of the surface. The sustained reaction is probably due to the formation of a mixed iron-aluminum mixed phosphate, which has been postulated to have both redox and strong acid-base sites.¹⁸ The reactivity of this material may, however, decay at longer times as found by Cao et al. because of poisoning by P₂O₅.

Comparison with Other Studies. As was mentioned in the Introduction, only one discussion of the quantitative decomposition of DMMP has been occurred in the literature at temperatures as low as 100 °C, and that measurement showed no product formation. In their work, Lee et al.⁴ stated that 100% DMMP conversion was obtained for their Cu-exchanged hydroxyapatite (Cu2-HA) at 100 °C for 5 min, a total flow of 86.5 μmol of DMMP converted for 0.3 g of solid (288 μmol of DMMP converted/g). As indicated in this work and by our earlier infrared studies,^{16,17} significant amounts of molecular DMMP are adsorbed on many oxide surfaces at temperatures as high as 100 °C, and the determination of decomposition needs to be confirmed by the measurement of products from the decomposition. By way of comparison, at the observed BTP in the current study at 100 °C, the commercial γ-Al₂O₃ had converted the equivalent of 238 μmol of DMMP/g of solid, as determined from the decomposition products, and the sol-gel Al₂O₃ had converted the equivalent of 517 μmol of DMMP/g of solid. At 200 °C, the lowest temperature reported for DMMP decomposition by Li and Klabunde,¹¹ their nanoscale MgO material converted the equivalent of 260 μmol of DMMP/g of solid, while the commercial alumina in this study converted the equivalent of 455 μmol of DMMP/g of solid at the BTP and the sol-gel alumina converted 1.12 mmol/g. Adding 2 wt % platinum to alumina significantly increases the activity as well as the cost for DMMP decomposition, so that Tzou and Weller observed a decomposition capacity of 2.19 mmol of DMMP/g of solid for their 2 wt % Pt/Al₂O₃ material at 150 °C.³

At somewhat higher temperatures, at 300 °C, the Cu2-HA material of Lee et al. converted, at the BTP, the equivalent of 577 μmol of DMMP/g of solid, while the commercial γ-Al₂O₃ has converted 1.25 mmol of DMMP/g, and the sol-gel alumina has converted 1.65 mmol of DMMP/g (these calculations assume that all of the DMMP has been converted up to the BTP since more than one volatile carbon molecule per DMMP has been produced). The nanoscale MgO results reported by Li and Klabunde showed a decomposition capacity of 960 μmol of DMMP/g of solid. At 250 °C, the 0.5 wt % Pt/Al₂O₃ material examined by Tzou and Weller showed a decomposition capacity of 19.9 mmol/g and the 2 wt % Pt material showed a decomposition capacity of 30.2 mmol/g, more than an order of magnitude higher than the other, non-Pt-containing solids.

At 400 °C, the presence of the copper and the oxidizing atmosphere begins to have an effect in the study of the copper-substituted hydroxyapatite material. The Cu2-HA material converted the equivalent of 4.33 mmol of DMMP/g of material at the BTP, while the commercial

(18) Gadgil, M. M.; Kulshreshtha, S. K. *J. Solid State Chem.* **1994**, *113*, 15.

alumina converted only 2.25 mmol/g and the sol-gel alumina converted only 3.37 mmol/g, although these latter two studies were in the absence of oxygen.

Recent studies of materials for the high-temperature decomposition of DMMP have included those by Cao et al.⁵ and Jiang et al.¹³ The vanadium on alumina material examined by Cao et al. showed a decomposition capacity of 20.2 mmol/g of solid and the iron oxide coated MgO nanoparticle material investigated by Jiang et al. decomposed the equivalent of 12.5 mmol/g of the solid at 500 °C. The 0.5 wt % Pt/Al₂O₃ material studied by Tzou and Weller showed a capacity of more than 54 mmol/g at 400 °C (they did not reach the BTP after 135 h).

Decomposition at Ambient Temperature. The reactivity of the solids at room temperature is dependent on the reactivity of the surface sites and their ability to convert DMMP to a chemisorbed species. Extensive experiments that will be reported in a future publication have shown that the presence or absence of oxygen in the atmosphere makes no measurable difference in either the overall product yield or the product branching ratios. Also, there is not enough thermal energy available to accomplish the rearrangement necessary to make the formation of bulk phosphate a reasonable possibility at ambient temperature in the absence of an additional energy source. Thus, for application as sorbent decontamination materials for chemical warfare agents, those materials that have the most active surface sites, even though they may not show sustained activity at high temperature, will be the most desirable, and the upper limit for the decomposition capacity will be determined by the number of available surface sites that actively decompose the agents.

The room-temperature adsorption/decomposition results can be used to form an estimate of the surface capacity and reactivity of the current materials for DMMP. For the commercial γ -Al₂O₃, for example, it appears from Figure 2A that the decomposition reaction was virtually complete by the time the sample had been exposed to 85 μ mol of DMMP, indicating that nearly all of the decomposition sites had been poisoned at this point. However, breakthrough of DMMP was observed much earlier, after exposure to 49 μ mol of DMMP. Up until breakthrough of DMMP, all of the inlet DMMP was adsorbed on the surface. After breakthrough, a decreasing fraction of the inlet DMMP was adsorbed, and methanol was produced at the sites that are active for decomposition, until all of the adsorption sites are saturated, which presumably also corresponds to the point at which all the decomposition sites have been poisoned. Thus, saturation coverage of the surface corresponds to between 49 and 85 μ mol of DMMP.

Using the Lewis acid site densities for dehydroxylated alumina reported by Knözinger and Ratnasamy,¹⁹ it can be calculated that 60 mg of the pure alumina (148 m²/g) should have an adsorption capacity of ≈ 75 μ mol of DMMP when dehydroxylated at 470 °C, assuming coordination through the P=O bond at Lewis acid sites (5.05×10^{14} sites/cm²). This is consistent with the estimate above of the saturation coverage of DMMP on the alumina surface.

Approximately 7 μ mol of volatile carbon are produced by the γ -Al₂O₃, and between 49 and 85 μ mol of DMMP is the estimated adsorption capacity. This yields an estimate of 8–14% for the fraction of adsorption sites that are active for decomposition. If the same adsorption site density is used for the FeO_x/Al₂O₃ surface (5.05×10^{14} sites/cm²), the predicted adsorption capacity for 60 mg is 53 μ mol of DMMP, which agrees with the observed DMMP breakthrough point. The total volatile carbon produced is ≈ 5.6 μ mol, so that the apparent fraction of adsorption sites that are active for decomposition is $\approx 10\%$, within the range of values estimated for γ -alumina at 25 °C.

The specific total product yield for the sol-gel alumina is higher than that of the other solids, as discussed above (see Figure 10). It is suspected that the presence of transitional phases in the sol-gel material is responsible for the higher reactivity of the surface. This defect site density may be one of the keys to forming the most active material for ambient temperature decomposition.

Conclusion

We have examined the adsorption and decomposition reaction of DMMP on three different materials from ambient temperature to 400 °C. For all three materials the following trend in behavior is observed. A low-temperature decomposition pathway is active at temperatures as low as 25 °C, whose rate increases with temperature. The reaction is poisoned by DMMP fragments and/or molecular DMMP, making the reaction stoichiometric, not catalytic, at these temperatures, and $\approx 10\%$ of the DMMP that is adsorbed will be decomposed via this path at 25 °C. Increasing temperature brings about an increase in the decomposition activity of the surface because of higher reactivity of the surface and less poisoning by molecular DMMP. This decomposition path is augmented at temperatures in excess of 200 °C by a reaction that involves continuous decomposition of DMMP. Since it is clear from numerous studies that DMMP fragments, primarily methyl methylphosphate, occupy all of the most active sites on the surface at these temperatures, this second reaction may involve participation of DMMP fragments directly in the continued decomposition.

At 200 °C, the sol-gel Al₂O₃ surface decomposes every DMMP molecule up to the BTP to yield, on average, one methanol molecule and one adsorbed fragment. At 300 °C, the BTP is 40% higher than at 200 °C, and every DMMP molecule up to the BTP decomposes to yield two methanol molecules, or the equivalent, and an adsorbed fragment.

At temperatures in excess of 300 °C, an additional set of products is observed, CO, CO₂, and CH₄. These species may be generated from the initial decomposition products of DMMP, methanol, or dimethyl ether, rather than from DMMP directly.

Acknowledgment. The authors would like to thank the U.S. Army, Edgewood Chemical Biological Center, for support of this research through Contract DAAD13-99-C-0010. Also, the authors would like to acknowledge the support of NASA through Grant NCC3-552.

(19) Knozinger, H.; Ratnasamy, P.; *Catal. Rev.-Sci. Eng.* **1978**, *17*, 31.